Fermilab

Observable CMB Tensor Modes from Cosmological Phase Transitions

FERMILAB-PUB-24-0752-T

arXiv:2410.23348

Observable CMB Tensor Modes from Cosmological Phase Transitions

Kylar Greene [1, 2, *] Aurora Ireland [3, †] Gordan Krnjaic [2, 4, 5, ‡] and Yuhsin Tsai [6, §]

[1] *Department of Physics and Astronomy, University of New Mexico Albuquerque, New Mexico 87131*
[2] *Theoretical Physics Division, Fermi National Accelerator Laboratory, Batavia, Illinois 60510*
[3] *Stanford Institute for Theoretical Physics, Department of Physics, Stanford University, Stanford, CA 94305*
[4] *Kavli Institute for Cosmological Physics, University of Chicago, Chicago, IL 60637*
[5] *Department of Astronomy and Astrophysics, University of Chicago, Chicago, IL 60637*
[6] *Department of Physics and Astronomy, University of Notre Dame, South Bend, IN 46556*

(Dated: November 1, 2024)

A B-mode polarization signal in the cosmic microwave background is widely regarded as smoking gun evidence for gravitational waves produced during inflation. Here we demonstrate that tensor perturbations from a cosmological phase transition in the post-inflationary universe can nearly mimic the characteristic shape and power of inflationary predictions across a range of observable angular scales. Although phase transitions arise from subhorizon physics, they nevertheless exhibit a white noise power spectrum on superhorizon scales. Thus, while B-mode power is suppressed on these large scales, it is not necessarily negligible. For viable phase transition parameters, the maximal B-mode amplitude at multipole moments around the recombination peak ($\ell \sim 100$) can be comparable to nearly all single-field inflationary predictions that can be tested with current and future experiments. This approximate degeneracy can be broken if a signal is measured at different angular scales, since the inflationary power spectrum is nearly scale invariant while the phase transition predicts a distinct suppression of power on large scales.

I. INTRODUCTION

Cosmological inflation is a compelling framework for dynamically solving the horizon and flatness problems while also generating the density perturbations observed in our universe today [1, 2]. Inflationary models also generically predict nearly scale-invariant tensor perturbations, which induce a characteristic B-mode polarization signal in the cosmic microwave background (CMB) [3–14]. It is widely accepted that observing B-modes above known astrophysical foregrounds would constitute "smoking gun" evidence for inflation [15–18].

In this *Letter*, we present a counterexample of post-inflationary B-modes that mimic the inflationary prediction. Indeed, *any* source of large-scale, coherent tensor perturbations produced before reionization can contribute to B-mode signals.[1] Our representative example is a late-time ($T \sim$ keV) strongly first-order phase transition, which produces gravitational waves (GWs) through bubble collisions, sound waves, and turbulence. The key difference with respect to the inflationary signal is that the spectrum from these subhorizon sources is not (nearly) scale invariant, but rather white noise on superhorizon scales. Accurately measuring B-modes on different angular scales can then in principle distinguish between these sources.

Pioneering earlier work has extensively studied the GW signal from cosmological phase transitions [20–53], with recent developments presenting analytical estimates of the GW signal [54–56]. Recently, it has also been shown that the white noise scalar perturbations from bubble nucleation can affect CMB temperature anisotropy measurements [57]. To our knowledge, however, the CMB B-mode signal from a first-order phase transition has not been calculated.

This *Letter* is organized as follows: Sec. II develops the formalism for calculating the B-mode polarization signal; Sec. III reviews the tensor power spectrum from a phase transition; Sec. IV presents our numerical results; Sec. V discusses the complimentary GW signal; and Sec. VI offers some concluding remarks and future directions.

II. B-MODE POLARIZATION

Tensor perturbations lead to temperature anisotropies in the CMB. When photons scatter with free electrons, quadrupole anisotropies in the temperature distribution are transformed into polarization of the scattered photons. The majority of CMB polarization is generated during recombination, since afterwards the number density of free electrons drops sharply and Thomson scattering ceases to be efficient. Here, we make the simplifying assumption that all polarization is generated in this last scattering event. This approximation will be relaxed in Sec. III, where we compute the angular B-mode spectrum exactly using the Boltzmann solver `CLASS` [58, 59]. The purpose of these formulas is simply to provide intuition as well as a semi-analytic check of our results.

Consider initially unpolarized photons which arrive along direction $\hat{n}'$ to the point $\vec{x}$, where they last scatter at conformal time τ. Letting $\hat{n}$ be the direction of

* kygreene@unm.edu
† anireland@stanford.edu
‡ krnjaicg@uchicago.edu
§ ytsai3@nd.edu

[1] See also Ref. [19] for B-mode signals from resonant particle production near reionization.

observation and τ_0 be the conformal time today, we can write $\vec{x} = (\tau_0 - \tau)\hat{n}$. A tensor perturbation $h_{ij}(\tau, \vec{k})$ gives the following contribution to the temperature anisotropy $\Theta \equiv \Delta T/T$, which can be written [60]

$$\Theta(\tau, \vec{k}; \hat{n}, \hat{n}') = \frac{1}{2}\int_0^\tau d\tau_1\, V(\tau, \tau_1) e^{i\vec{k}\cdot\hat{n}(\tau_0-\tau)} \times \int_{\tau_1}^\tau d\tau_2 e^{-i\vec{k}\cdot\hat{n}'(\tau-\tau_2)} \sum_{\lambda=+,\times} n_i' \epsilon_{ij}^\lambda n_j'\, \partial_{\tau_2} h_\lambda(\tau_2, \vec{k}) \quad (1)$$

where ϵ_{ij}^λ is the polarization tensor for gravitational waves, the sum runs over graviton polarizations, and $V(\tau_1, \tau_2)$ is the visibility function, which satisfies

$$V(\tau_1, \tau_2) = e^{-\kappa(\tau_1,\tau_2)} \frac{d\kappa(\tau_2)}{d\tau_2}\,, \quad (2)$$

and is defined in terms of the optical depth

$$\kappa(\tau_1, \tau_2) = \int_{\tau_2}^{\tau_1} d\tau\, a(\tau)\, \sigma_T\, n_e(\tau) \quad (3)$$

where n_e is the electron number density and σ_T is the Thomson cross section. This temperature anisotropy gives rise to an anistropy in the intensity of incoming radiation, and so Θ enters into the CMB polarization tensor as [3, 60]

$$P_{ab}(\vec{k}; \hat{n}) = \frac{3}{4\pi}\int d^2n'\varepsilon_{ab}\int_0^{\tau_0} d\tau V(\tau_0, \tau)\Theta(\tau, \vec{k}; \hat{n}\cdot\hat{n}'), \quad (4)$$

and we have defined the tensor

$$\varepsilon_{ab} = \frac{1 - (\hat{n}\cdot\hat{n}')^2}{2} g_{ab} - \hat{n}'\mathbf{e}_a \cdot \hat{n}'\mathbf{e}_b\,, \quad (5)$$

where $\mathbf{e}_a$ is the set of basis vectors on the celestial sphere and g_{ab} is the background metric. Notice that because $\hat{n}'$ enters in a bilinear combination, polarization requires a quadrupole component to the anisotropy.

It is convenient to decompose the polarization tensor into E- and B-modes, which can each be expanded in spherical harmonics on the celestial sphere. Doing so, one can identify the coefficient

$$a^B_{\ell m}(\vec{k}) = -\int d^2n \left[Y^{(B)}_{\ell m}\right]^*_{ab}(n)\, P^{ab}(\vec{k}; \hat{n})\,, \quad (6)$$

where $Y^{(B)}_{\ell m}$ are the B-mode tensor harmonics on the sphere.[2] The angular spectrum of B-mode polarization is defined in terms of these coefficients as

$$C_\ell^{BB} = \frac{1}{2\ell+1}\sum_{m=\pm 2}\int \frac{d^3k}{(2\pi)^3}\left\langle a^B_{\ell m}(\vec{k})\, a^B_{\ell m}(\vec{k})^*\right\rangle\,, \quad (8)$$

where the angle brackets denote ensemble average. Working in a frame with the azimuthal axis oriented along $\vec{k}$ to perform the integrals, one can show that

$$C_\ell^{BB} = 36\pi\int_0^\infty \frac{dk}{k}\mathcal{P}_h(k)\mathcal{F}_\ell(k)^2\,, \quad (9)$$

where $\mathcal{P}_h(k)$ is the dimensionless tensor power spectrum evaluated at the initial time and

$$\mathcal{F}_\ell(k) = \int_0^{\tau_0} d\tau\, V(\tau_0, \tau)\, \mathcal{S}_\ell(k, \tau_0, \tau)\int_0^\tau d\tau_1\, V(\tau, \tau_1) \times \int_{\tau_1}^\tau d\tau_2\, \frac{j_2[k(\tau-\tau_2)]}{k^2(\tau-\tau_2)^2}\left(\frac{\partial\mathcal{T}(\tau_2, k)}{\partial\tau_2}\right), \quad (10)$$

where we have defined

$$\mathcal{S}_\ell(k, \tau_0, \tau) \equiv \frac{\ell+2}{2\ell+1} j_{\ell-1}[k(\tau_0-\tau)] - \frac{\ell-1}{2\ell+1} j_{\ell+1}[k(\tau_0-\tau)]. \quad (11)$$

Note that in deriving this result, we have decomposed the tensor perturbation into an initial perturbation amplitude $h_\lambda^{\rm ini}(k)$ and the transfer function $\mathcal{T}(\tau, \vec{k})$, where

$$h_\lambda(\tau, \vec{k}) = h_\lambda^{\rm ini}(\vec{k})\mathcal{T}(\tau, \vec{k})\,. \quad (12)$$

This decomposition is useful because it separates the effect of statistical correlations between the initial amplitudes from the deterministic effect of the modes' subsequent evolution, as captured by the transfer function. The statistical properties of the initial perturbations are encoded in the (dimensionful) power spectrum $P_h(k)$,

$$\left\langle h_\lambda^{\rm ini}(\vec{k})\, h_{\lambda'}^{\rm ini}(\vec{k}')^*\right\rangle = \frac{\delta_{\lambda\lambda'}}{2} P_h(k)(2\pi)^3\delta^{(3)}(\vec{k} - \vec{k}')\,. \quad (13)$$

We also introduce the dimensionless power spectrum appearing in Eq. (9),

$$\mathcal{P}_h(k) = \frac{k^3}{2\pi^2} P_h(k)\,. \quad (14)$$

In the presence of a nonzero source $\Pi_{ij}(\tau, \vec{k})$, a Fourier mode of the metric perturbation $h_{ij}(\tau, \vec{k})$ evolves according to the wave equation

$$h_{ij}'' + 2\mathcal{H}h_{ij}' + k^2 h_{ij} = 8\pi G a^2 \Pi_{ij}\,, \quad (15)$$

where $\mathcal{H} = a'/a$ is the conformal Hubble rate, primes denote derivatives with respect to conformal time, and the source term is the Fourier transformed anisotropic stress. When the source is inactive, the transfer function satisfies

$$\mathcal{T}'' + 2\mathcal{H}\mathcal{T}' + k^2\mathcal{T} = 0\,. \quad (16)$$

Following Ref. [61], we ignore the late-time contribution from dark energy, and consider only effects from the transition from radiation to matter domination. In this 2-component universe, the Friedman equations can be

[2] The B-mode tensor harmonics are related to the ordinary spherical harmonics as

$$\left(Y^{(B)}_{\ell m}\right)_{ab}(n) = \sqrt{\frac{(\ell-2)!}{2(\ell+2)!}}\left(\epsilon_b^c\nabla_a\nabla_c + \epsilon_a^c\nabla_c\nabla_b\right) Y_{\ell m}(n)\,. \quad (7)$$

solved analytically, and one can derive the following solutions for the transfer function in the radiation-dominated and matter-dominated regimes

$$\mathcal{T}_{\rm RD}(\tau,k) = A_k\, j_0(k\tau) - B_k\, y_0(k\tau) \quad (17)$$

$$\mathcal{T}_{\rm MD}(\tau,k) = \frac{3}{k\tau}\left[C_k\, j_1(k\tau) - D_k\, y_1(k\tau)\right]. \quad (18)$$

From the initial conditions and the matching conditions at the characteristic timescale $\tilde{\tau} = 4\sqrt{\Omega_r}/H_0\Omega_m$, the constants in Eq. (17) are $A_k = 1, B_k = 0$, and those in Eq. (18) satisfy

$$C_k = \frac{1}{2} - \frac{\cos(2k\tilde{\tau})}{6} + \frac{\sin(2k\tilde{\tau})}{3k\tilde{\tau}}\,,$$
$$D_k = -\frac{1}{3k\tilde{\tau}} + \frac{k\tilde{\tau}}{3} + \frac{\cos(2k\tilde{\tau})}{3k\tilde{\tau}} + \frac{\sin(2k\tilde{\tau})}{6}\,. \quad (19)$$

Given a form for the initial tensor power spectrum, Eq. (9) in conjunction with Eqs. (10), (17), (18), and (19) can be used to compute the B-mode signal. These expressions contain many nested integrals with oscillatory integrands, however, which can lead to numerical instabilities. Approximating the visibility function as a Gaussian of width $\Delta\tau_r \simeq 0.04\tau_r$ about its maximum [60], the conformal time integrals can be simplified considerably to yield

$$C_\ell^{BB} \simeq \frac{36\pi}{25}\left(\frac{\Delta\tau_r}{\tau_r}\right)^2 \int_0^\infty \frac{dk}{k}\mathcal{P}_h(k)\, j_2(k\tau_r)^2 \mathcal{S}_\ell(k,\tau_0,0)^2, \quad (20)$$

where we have used the fact that modes entering during matter domination ($\tau > \tau_{\rm eq}$) obey

$$\mathcal{T}(\tau,k) \to \frac{3j_1(k\tau)}{k\tau}. \quad (21)$$

Note that the approximation in Eq. (20) is inadequate to properly capture the behavior of C_ℓ^{BB} for large multipoles $\ell \gtrsim 100$. For this reason, we will use exclusively Eq. (9) when comparing our numerical results against these semi-analytic expectations in Sec. IV.

III. TENSOR POWER SPECTRUM FROM BUBBLE COLLISIONS

We consider first-order cosmological phase transitions in the post-inflationary universe as an example of a source of large-scale, coherent tensor perturbations. Such phase transitions proceed through bubble nucleation, which sources tensor perturbations in three distinct stages.

During the bubble collision stage, bubbles of true vacuum collide and merge, breaking spherical symmetry and allowing the gradient energy of the scalar field to source anisotropies [62, 63]. This phase completes quickly; nevertheless, it can be the dominant contribution for strong vacuum transitions. After the bubbles have merged, shells of fluid kinetic energy continue to propagate through the plasma, colliding and sourcing GWs during the acoustic stage [31, 64, 65]. These sound wave collisions can produce vorticity, turbulence, and shocks in the fluid, which in turn source GWs during the turbulent stage [66–69].

The relative contribution from each of these stages depends largely on the transition strength, as parameterized by α, as well as the bubble wall velocity v_w. For concreteness, we will consider a near-vacuum transition with runaway bubble wall, for which the dominant contribution comes from the bubble collision stage. Thus we consider *only* the contribution from this stage. In deriving the initial tensor power spectrum of this source, we follow the semi-analytic approach of Refs. [54, 55]. During the phase transition, we solve Eq. (15) with source term $\Pi_{ij}(\tau,\vec{k})$, defined as the Fourier transform of the anisotropic stress — the transverse, traceless part of the energy-momentum tensor

$$\Pi_{ij}(\tau,\vec{k}) = \left(\pi_{ik}\pi_{jl} - \frac{1}{2}\pi_{ij}\pi_{kl}\right) T_{kl}(\tau,\vec{k})\,, \quad (22)$$

with $\pi_{ij} = \delta_{ij} - \hat{k}_i\hat{k}_j$. We take the source to be a statistically homogeneous, isotropic random variable with unequal-time correlator

$$\left\langle \Pi_{ij}(\tau_1,\vec{k})\Pi^*_{ij}(\tau_2,\vec{k}')\right\rangle = (2\pi)^3\delta^{(3)}(\vec{k}-\vec{k}')\Pi(\tau_1,\tau_2,k). \quad (23)$$

We also assume the phase transition is short-lived and completes within a fraction of a Hubble time $H_* \ll \beta$, where β is the inverse duration of the phase transition.

To solve Eq. (15), we introduce the comoving tensor perturbation $\mathfrak{h}_{ij}(\tau,\vec{k}) \equiv a(\tau)h_{ij}(\tau,\vec{k})$, whose wave equation is

$$\mathfrak{h}''(\tau,\vec{k}) + \left(k^2 - \frac{a''}{a}\right)\mathfrak{h}(\tau,\vec{k}) = 8\pi G a^3 \Pi_{ij}(\tau,\vec{k})\,. \quad (24)$$

We also introduce the Green's function $G_k(\tau,\bar{\tau})$, which solves the homogeneous equation with delta function source and boundary conditions $G_k(\tau,\tau) = 0$, $G'_k(\tau,\bar{\tau})|_{\tau=\bar{\tau}} = 1$. During radiation domination $a \propto \tau$, so $a'' = 0$ and we have

$$G_k(\tau,\bar{\tau}) = \frac{\sin[k(\tau-\bar{\tau})]}{k}\,. \quad (25)$$

The solution for $\mathfrak{h}_{ij}(\tau,k)$ during the phase transition $\tau \in [\tau_i,\tau_f]$ is given by convolution

$$\mathfrak{h}_{ij}(\tau,\vec{k}) = 8\pi G\int_{\tau_i}^{\tau} d\tau_1\, G_k(\tau,\tau_1) a_1^3 \Pi_{ij}(\tau_1,\vec{k})\,, \quad (26)$$

where $a_j = a(\tau_j)$. At the end of the transition, the initial tensor mode amplitude $h_{ij}^{\rm ini}(\vec{k}) \equiv h_{ij}(\tau_f,\vec{k})$ is then

$$h_{ij}^{\rm ini}(\vec{k}) = \frac{8\pi G}{a_f k}\int_{\tau_i}^{\tau_f} d\tau_1 \sin[k(\tau_f-\tau_1)]\, a_1^3\, \Pi_{ij}(\tau_1,\vec{k})\,. \quad (27)$$

Substituting this explicit solution into Eq. (13) and summing over polarizations, the initial power spectrum is

$$P_h = \frac{32\pi^2 G^2}{a_f^2 k^2}\int_{\tau_i}^{\tau_f} d\tau_1 \int_{\tau_i}^{\tau_f} d\tau_2 \cos[k(\tau_1-\tau_2)]\tilde{\Pi}(\tau_1,\tau_2,k)\,, \quad (28)$$

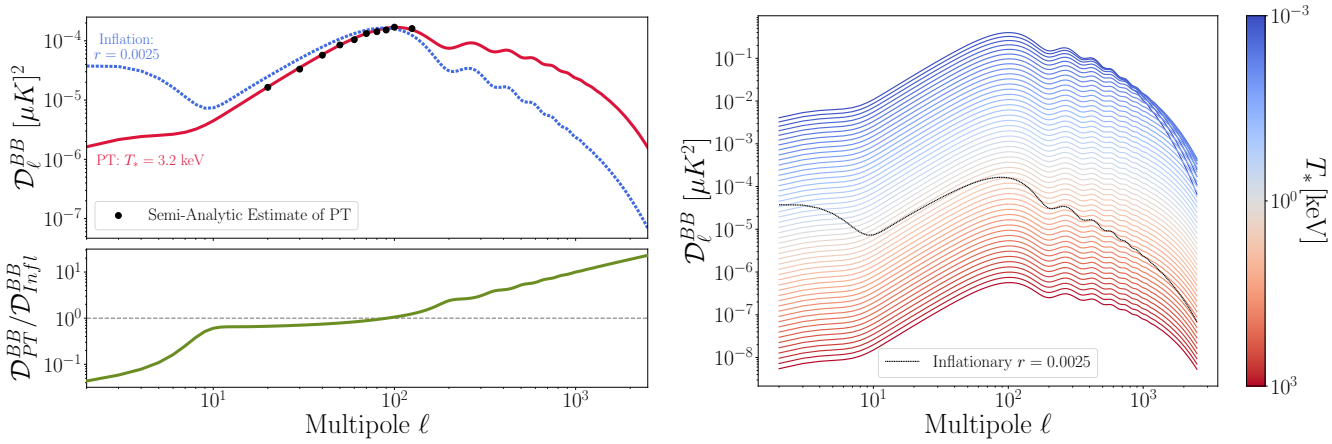

FIG. 1: **Left Top**: B-mode polarization spectra for a phase transition with parameters $T_* = 3.2$ keV, $\kappa = 1$, $\alpha = 0.039$, and $\beta/H = 10$ (solid red) and a minimal inflationary model with $r = 0.0025$ (dashed blue). Semi-analytic prediction of Eq. (9) shown for comparison (black points). Parameters chosen to saturate bounds from $\Delta N_{\rm eff}$ and finite bubble statistics. Lensing removed for illustrative purposes. **Left Bottom**: Ratio of B-mode signals from these sources. **Right**: Contours of B-mode spectra for phase transitions at different values of T_*. Other parameters same as left panel. Inflationary prediction for $r = 0.0025$ shown for comparison (black). Note that phase transition temperatures with peak power above the $r = 0.0025$ curve are ruled out for the specific model considered, based on the constraints of Fig. 2.

where $\tilde{\Pi}(\tau_1,\tau_2,k) \equiv a_1^3 a_2^3 \Pi(\tau_1,\tau_2,k)$ and the unequal-time correlator is defined in Eq. (23). Since we assume the phase transition completes in well under a Hubble time, we can neglect expansion while the source is active and approximate all insertions of the scale factor with the same constant value during the phase transition, $a_i \approx a_f \equiv a_*$. In this limit, Eq. (28) simplifies to

$$P_h \simeq \frac{32\pi^2 G^2 a_*^4}{k^2} \int_{\tau_i}^{\tau_f} d\tau_1 \int_{\tau_i}^{\tau_f} d\tau_2 \cos[k(\tau_1-\tau_2)] \Pi(\tau_1,\tau_2,k)\,. \quad (29)$$

Note that this double integral has the same form as Eq. (23) of Ref. [55], which identified the result with the dimensionless quantity $\Delta(k/\beta)$,

$$\int_{t_i}^{t_f} dt_1 \int_{t_i}^{t_f} dt_2 \cos[k(t_1-t_2)]\, \Pi(t_1,t_2,k) \equiv \frac{3\kappa^2 H_*^4}{16 G^2 \beta^2 k^3} \left(\frac{\alpha}{1+\alpha}\right)^2 \Delta\left(\frac{k}{\beta}\right), \quad (30)$$

where the transition strength α describes the ratio of vacuum energy released relative to that in radiation, and the efficiency factor κ characterizes how much vacuum energy goes into bulk kinetic energy. Note that $\Delta(k/\beta)$ depends only[3] on the ratio k/β, since other thermal phase transition parameters have been factored out.

In order to express our result in terms of this Δ function, note that Ref. [55] carries out their source calculation integrating over the dimensionless quantity $t\beta$ (where they have set $\beta = 1$ in all intermediate steps). Since we work in conformal time, the corresponding dimensionless quantity for us is $\tau a_* \beta$. Thus, we are justified in using their functional form for Δ with the replacement $\beta \to a_* \beta$, so that the dimensionless tensor power spectrum becomes

$$\mathcal{P}_h(k) = 3\kappa^2 \left(\frac{a_* H_*}{k}\right)^2 \left(\frac{H_*}{\beta}\right)^2 \left(\frac{\alpha}{1+\alpha}\right)^2 \Delta\left(\frac{k}{a_*\beta}\right). \quad (31)$$

Note that the semi-analytical Δ calculation in Ref. [55] uses the thin wall and envelope approximations and we show the complete expression in Appendix B. This result can be approximated with an empirical fitting formula, which reproduces the full spectrum to within 8% error [55]

$$\Delta(x) \simeq \Delta_p \left[c_l x^{-3} + (1 - c_l - c_h) x^{-1} + c_h x\right]^{-1}, \quad (32)$$

where $x \equiv k/k_p$, $k_p \simeq 1.24\, a_* \beta$ is the peak frequency of the phase transition, $\Delta_p \simeq 0.043$ is the peak amplitude, $c_l \simeq 0.064$, and $c_h \simeq 0.48$. The most important thing to note is that the high- and low-k scaling of Δ is

$$\Delta \propto \begin{cases} k^3 & k/(a_*\beta) \lesssim 1 \\ k^{-1} & k/(a_*\beta) \gtrsim 1 \end{cases}. \quad (33)$$

In particular, the low-frequency regime displays the expected k^3 behavior characteristic of the causality-limited part of a stochastic GW spectrum — that is, those modes whose wavelengths (and periods) are much larger than the spatial (and temporal) correlations of the source [70]. This result in conjunction with the k-scaling of $\mathcal{P}_h$ in

[3] In principle, Δ also depends on the wall velocity v_w. We follow Ref. [55] in setting $v_w = 1$ for simplicity.

Eq. (31) implies

$$\mathcal{P}_h \propto \begin{cases} k & k/(a_*\beta) \lesssim 1 \\ k^{-3} & k/(a_*\beta) \gtrsim 1 \end{cases} . \tag{34}$$

Naively, the B-mode contribution from cosmological phase transitions should be negligible since the CMB is sensitive to long-wavelength modes and the phase transition power spectrum is suppressed at low frequencies. The mildness of this $\mathcal{P}_h \sim k$ fall-off suggests, however, that for sufficiently strong transitions, the power in the causal tail may still be appreciable enough to yield an observable B-mode signal.

IV. NUMERICAL RESULTS

In Fig. 1, we plot the angular B-mode power spectrum in terms of

$$\mathcal{D}_\ell^{BB} \equiv \frac{\ell(\ell+1)}{2\pi} T_0^2 C_\ell^{BB} , \tag{35}$$

with C_ℓ^{BB} defined in Eq. (8). The left panel compares the numerically calculated $\mathcal{D}_\ell^{BB}$ spectra for two scenarios:

- A phase transition with parameters $T_* = 3.2\,\text{keV}$, $\kappa = 1$, $\alpha = 0.039$, and $\beta/H_* = 10$ chosen to saturate bounds from ΔN_{eff} [71] and finite bubble statistics [57]. This benchmark point corresponds to the blue star in Fig. 2
- A minimal inflationary model with a tensor-to-scalar ratio of $r = 0.0025$, selected to match the peak amplitude of the phase transition signal at the multipole $\ell \approx 100$.

For illustrative purposes, we exclude the predicted lensing signal from both cases to highlight the shape differences between these sources. Note that the lensing signal is a foreground effect that impacts both models in a similar way [72–83].

The solid and dashed curves in the top left panel are computed using the Boltzmann solver `CLASS` [59]. In particular for the phase transition signal, we utilize the `external-pk` module with the custom primordial tensor power spectrum from Eq. (13). `CLASS` then computes the transfer functions from the Einstein-Boltzmann equations and the polarization source functions. These outputs, combined with the primordial tensor power spectrum, are then used to evaluate the line-of-sight and k-space integrals to obtain the C_ℓ^{BB}. For comparison, we show also the semi-analytic estimate from Eq. (9), which accurately captures the recombination peak but becomes numerically challenging at higher multipoles $\ell > 100$. In contrast, `CLASS` efficiently handles the numerical integration required at higher multipoles.

The bottom left panel shows the ratio of the phase transition and inflationary B-mode predictions, highlighting their distinct spectral shapes. The tensor power spectrum from a phase transition scales as $\mathcal{P}_h(k) \propto k$ in the superhorizon regime, resulting in enhanced power at higher multipoles and suppressed power at lower multipoles compared with the nearly scale-invariant inflationary case. In particular, the reionization peak at $\ell \lesssim 10$ is essentially absent in the phase transition spectrum. The difference in the distribution of power across angular scales implies that these scenarios can in principle be distinguished.

The right panel of Fig. 1 shows B-mode power spectra for various phase transition temperatures ranging from $T_* = 1$ eV to $T_* = 1$ MeV, whilst keeping $\kappa = 1$, $\alpha = 0.039$, and $\beta/H_* = 10$ fixed to their benchmark values. For comparison, we show also the inflationary prediction with $r = 0.0025$ (black), which is well within the sensitivity of future B-mode experiments such as LiteBIRD [88] and CMB-S4 [89]. Phase transitions at lower temperatures yield B-mode signals that can rival or even exceed those from inflation, emphasizing the importance of considering such alternatives in CMB analyses.

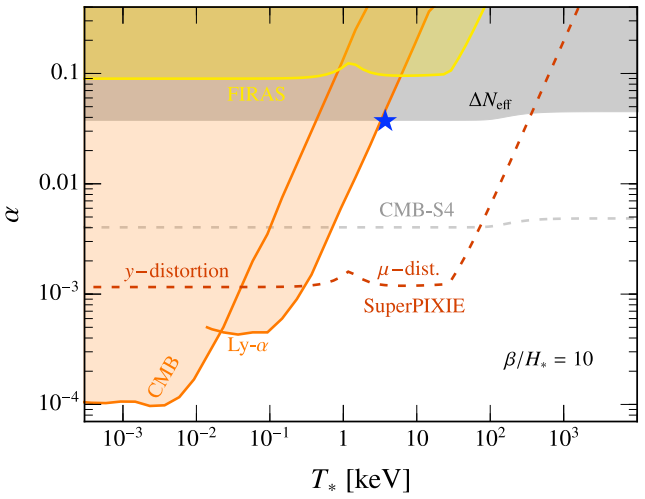

FIG. 2: Experimental limits (2σ) on α for various phase transition temperatures, assuming all energy is released into dark radiation (adapted from Ref. [57]). Here we show bounds from Lyman-α [84] (orange shaded), CMB scalar perturbations [85] (orange shaded), CMB spectral distortions COBE-FIRAS, [86] (yellow shaded), and the CMB limit on $\Delta N_{\text{eff}} \geq 0.29$ [71] (light grey shaded). We show also future projections from CMB-S4 (grey dashed curve) and SuperPIXIE [87] (red dashed curve), assuming sensitivity of $\Delta\rho_\gamma/\rho_\gamma \sim 10^{-8}$. The blue star denotes the benchmark point of Fig. 1, for which $\alpha = 0.039$, $\kappa = 1$, $v_w = 1$, $T_* = 3.2$ keV, and $\beta/H_* = 10$.

V. A COMPLEMENTARY GW SIGNAL

The tensor perturbations that source our B-modes also result in a stochastic GW background that offers a complementary signal of our scenario. The relative energy

density in GWs per logarithmic frequency interval is quantified by the spectral density parameter $\Omega_{\rm GW}$

$$\Omega_{\rm GW} = \frac{1}{\rho_{\rm tot}} \frac{d\rho_{\rm GW}}{d\ln k} \,. \tag{36}$$

At the time of the phase transition τ_*, the energy density in GWs is

$$\rho^*_{\rm GW} = \frac{1}{8\pi G a_*^2} \left\langle h'_{ij}(\tau_*, \vec{x}) h'_{ij}(\tau_*, \vec{x}) \right\rangle \,, \tag{37}$$

where the real-space correlation function can be expressed as

$$\left\langle h'_{ij}(\tau, \vec{x}) h'_{ij}(\tau, \vec{x}) \right\rangle = \int d\ln k \, \mathcal{P}_{h'}(\tau, k) \,. \tag{38}$$

Using the explicit form of h_{ij}, one can show that $\mathcal{P}_{h'}(k) = k^2 \mathcal{P}_h(k)$. From the above and Eq. (31), one can work out that at the time of the phase transition

$$\Omega^*_{\rm GW} = \kappa^2 \left(\frac{H_*}{\beta}\right)^2 \left(\frac{\alpha}{1+\alpha}\right)^2 \Delta\left(\frac{2\pi f_*}{\beta}\right) \,, \tag{39}$$

where as a last step we have introduced the physical frequency f, related to the comoving momentum as $k = 2\pi a f$.

To translate this signal to today, we can use entropy conservation relate the scale factor at the transition to that today

$$\frac{a_*}{a_0} = \left[\frac{g_{\star,s}(T_0)}{g_{\star,s}(T_*)}\right]^{1/3} \frac{T_0}{T_*} \,. \tag{40}$$

The frequency redshifts like one power of the scale factor, $f_0 = f_* \, (a_*/a_0)$, while the energy density in GWs dilutes as four powers of the scale factor, $\rho^0_{\rm GW} = \rho^*_{\rm GW} \, (a_*/a_0)^4$. The spectral density parameter today is then

$$\Omega_{\rm GW} h^2 \simeq 4 \times 10^{-5} \kappa^2 \alpha^2 \left(\frac{H_*}{\beta}\right)^2 \Delta\left(\frac{2\pi f_0}{a_* \beta}\right) \,, \tag{41}$$

where we have normalized $a_0 = 1$ and taken $g_\star(T_\star) = 3.36$ and $g_{\star,s}(T_\star) = 3.91$, since we focus on late-time phase transitions.

In Fig. 3, we show sample $\Omega_{\rm GW}$ predictions for the phase transition and inflationary scenarios, presented alongside the CMB constraints from Ref. [90]. As discussed in Appendix A, the precise location of the CMB limit from B-modes is model dependent, as translating sensitivity from $\mathcal{D}_\ell^{BB}$ to $\Omega_{\rm GW}$ depends on the power spectrum of the source. Because the phase transition only produces GWs at time τ_*, the corresponding GW spectrum picks up an additional suppression factor $(k\tau_*)^2 \sim 10^{-10}$ relative to the inflationary curve at frequencies near $f \sim 10^{-17}$ Hz, corresponding to scales $k \sim 10^{-2}\,{\rm Mpc}^{-1}$ — even though both signals have similar peak values in $\mathcal{D}_\ell^{\rm BB}$ at this scale.

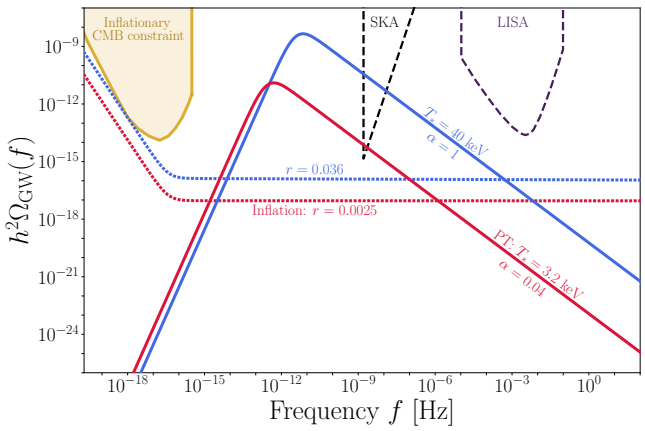

FIG. 3: Representative GW spectra for tensor modes from phase transitions (PT) (solid) and inflation (dotted), shown alongside the CMB constraint on inflation from Ref. [90]. The solid PT curves shown here predict the same B-mode power at $\ell = 100$ as the corresponding dotted inflationary curves of the same color. In Appendix A, we discuss the model dependence of this limit and why the CMB B-mode constraint for these PTs is actually much lower on this plane; calculating this limit beyond the scope of this work. The light blue inflation curve ($r = 0.036$) meets the BICEP upper limit [91] and matches the peak B-mode amplitude of a $T_* = 40$ keV PT with $\alpha = 1$, though ruled out by Fig. 2. Similarly, $r = 0.0025$ aligns with a $T_* = 3.2$ keV PT with $\alpha = 0.039$ (Fig. 1, upper left). Both PT curves assume $\kappa = 1$ and $\beta/H_* = 10$. Sensitivity curves for LISA (purple) [92] and SKA (black) [93] are also shown.

VI. DISCUSSION

In this *Letter*, we have found that the gravitational waves produced during a late-time, first-order phase transition can generate CMB B-modes on observable scales. Although phase transitions occur due to causal processes on subhorizon scales, they nonetheless exhibit white noise on large scales and the corresponding B-modes from this white noise power can viably mimic the more familiar inflationary signal across a range of multipole moments. Thus, a positive detection of B-modes beyond the known lensing effect is no longer a definitive "smoking gun" for inflation, though it is still clear evidence of new physics.

Fortunately, the phase transition signal is not fully degenerate with the inflationary predictions. Although the peak power from any testable inflationary model (down to $r \sim 10^{-3}$) can also be accommodated with a viable late-time phase transition, the latter signal exhibits a characteristic spectral shape: low-ℓ suppression and high-ℓ enhancement relative to the inflationary prediction. Thus, these hypotheses can ultimately be distinguished with sufficiently precise B-mode measurements on different angular scales scales. Furthermore, the cosmological

phase transitions we have considered may also predict stochastic GW backgrounds within SKA sensitivity [93], CMB spectral distortions observable with PIXIE [94] and SPECTER [95], and $\Delta N_{\rm eff}$ within the reach of CMB-S4 targets [89]. Collectively, these additional probes can, in principle, break the near degeneracy between the inflationary and phase transition B-mode signals.

Note that our treatment of gravitational waves from phase transitions is conservative as we have only included contributions from bubble collisions and omitted the effects of turbulence and sound waves. Furthermore, many of the limits on cosmological phase transitions (e.g. $\Delta N_{\rm eff}$) are model dependent as they assume a specific equation of state for the hidden sector after the transition completes. Fully accounting for these effects and their variations could allow for much louder GW signals within viable parameter space, but we leave a more detailed treatment for future work.

While our result heightens the challenge of understanding inflation from a B-mode discovery at a single angular scale, it also opens the door to understanding a wider range of new physics in the event of such a discovery. Indeed, we have shown that all existing and future experiments sensitive to B-modes can also be sensitive to white noise power from a new range of new, non-inflationary scenarios. We note that similar white noise signals may also arise from other sources, including cosmic strings or domain walls, whose contributions we leave for future work.

ACKNOWLEDGEMENTS

We would like to thank Adam Anderson, Francis-Yan Cyr-Racine, Scott Dodelson, Josh Foster, Peter Graham, Wayne Hu, Marc Kamionkowski, Gustavo Marques-Tavares, Jeff McMahon, Julian Muñoz, Albert Stebbins, Matthew Young, and Jessica Zebrowski for helpful conversations. AI is supported by NSF Grant PHY-2310429, Simons Investigator Award No. 824870, DOE HEP QuantISED award #100495, the Gordon and Betty Moore Foundation Grant GBMF7946, and the U.S. Department of Energy (DOE), Office of Science, National Quantum Information Science Research Centers, Superconducting Quantum Materials and Systems Center (SQMS) under contract No. DEAC02-07CH11359. Fermilab is operated by the Fermi Research Alliance, LLC under Contract DE-AC02-07CH11359 with the U.S. Department of Energy. This material is based partly on support from the Kavli Institute for Cosmological Physics at the University of Chicago through an endowment from the Kavli Foundation and its founder Fred Kavli. This material is based upon work supported by the U.S. Department of Energy, Office of Science, Office of Workforce Development for Teachers and Scientists, Office of Science Graduate Student Research (SCGSR) program. The SCGSR program is administered by the Oak Ridge Institute for Science and Education for the DOE under contract number DE-SC0014664. YT is supported by the NSF Grant PHY-2112540 and PHY-2412701. YT would like to thank the Tom and Carolyn Marquez Chair Fund for its generous support. YT would also like to thank the Aspen Center for Physics (supported by NSF grant PHY-2210452).

Appendix A: Model Dependence of CMB $\Omega_{\rm GW}$ limits

In this appendix, we derive the relationship between CMB limits on $\Omega_{\rm GW}$ for phase transitions and compare these limits to the more familiar inflationary case shown in Fig. 3. We first show that the primordial power spectra $\mathcal{P}_h(k)$ are approximately equal for a k value associated with the predicted peaks of the $\mathcal{D}_\ell^{\rm BB}$ spectra. We then demonstrate that these peaks are indeed nearly equivalent in amplitude in $\mathcal{D}_\ell^{\rm BB}$ space. Finally, using the same $\mathcal{P}_h(k)$ that produced similar $\mathcal{D}_\ell^{\rm BB}$ signals, we define the relationship between $\Omega_{\rm GW}^{\rm inf}$ and $\Omega_{\rm GW}^{\rm PT}$, demonstrating a relative suppression between the two predicted spectra on large scales, even though the $\mathcal{P}_h(k)$ which source them produce similar $\mathcal{D}_\ell^{\rm BB}$ amplitude at the given scale.

The inflationary prediction for the primordial tensor power spectrum is parameterized as

$$\mathcal{P}_h^{\rm inf}(k) = rA_{\rm s}\left(\frac{k}{k_{\rm piv}}\right)^{n_T}, \tag{A1}$$

where $A_s = 2.1\times10^{-9}$ is the amplitude of scalar fluctuations and $k_{\rm piv} = 0.05$ Mpc^{-1} is the pivot scale [71]. For illustration, let us consider the a minimal inflationary model with tilt $n_T = -r/8$ and a reference value for the tensor-to-scalar ratio which saturates the BICEP bound, $r = 0.036$ [91]. For phase transitions, the corresponding tensor power spectrum is given in Eq. (31),

$$\mathcal{P}_h^{\rm PT}(k) = 3\kappa^2\left(\frac{a_*H_*}{k}\right)^2\left(\frac{H_*}{\beta}\right)^2\left(\frac{\alpha}{1+\alpha}\right)^2\Delta\left(\frac{k}{a_*\beta}\right). \tag{A2}$$

We adopt the model parameters

$$\kappa = \alpha = 1 \quad , \quad \beta/H = 10 \quad , \quad T_* = 40\,{\rm keV}\,, \tag{A3}$$

so that the amplitude of $\mathcal{D}_\ell^{BB}$ at the $\ell\sim100$ peak roughly matches the amplitude of the inflationary signal.

The recombination peaks of the $\mathcal{D}_\ell^{\rm BB}$ spectra occur around $\ell\sim100$ for both the phase transition and inflationary signals. Using the approximation $\ell\sim k\tau_0$, this ℓ mode corresponds roughly to the comoving momentum $k_{100}\equiv 6.45\times10^{-3}$ Mpc^{-1} and the frequency $f\sim10^{-17}$ Hz. For the benchmark phase transition inputs from Eq. (A3), chosen so the two types of signals have similar power at k_{100}, we find

$$\mathcal{P}_h^{\rm inf}(k_{100}) \approx \mathcal{P}_h^{\rm PT}(k_{100}) \approx 9\times10^{-11}\,. \tag{A4}$$

The primordial tensor power spectrum gives the B-mode signal via

$$\mathcal{D}_\ell^{BB} = 18\ell(\ell+1)T_0^2\int_0^\infty\frac{dk}{k}\mathcal{P}_h(k)\mathcal{F}_\ell(k)^2\,, \tag{A5}$$

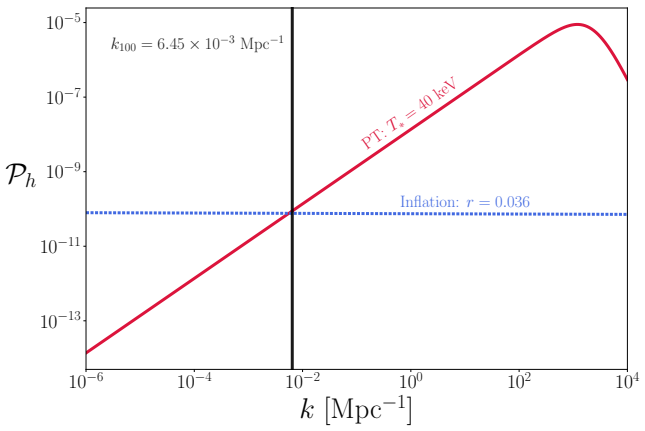

FIG. 4: Dimensionless tensor power spectra $\mathcal{P}_h(k)$ corresponding to a sample phase transition with parameters given in Eq. (A3) (solid red) and inflation with $r = 0.036$ (dotted blue). The vertical grey line denotes the comoving momentum associated with $\ell \sim 100$, for which the power spectra are approximately equal.

where $\mathcal{F}_\ell(k)^2$ is independent of the source of tensor perturbations and we have combined Eqs. (9) and (35). The similar $\mathcal{P}_h(k_{100})$ values for the two signals also yield similar peak values ($\ell \approx 100$) for the B-mode power

$$\mathcal{D}_{100}^{BB,\rm inf} \approx \mathcal{D}_{100}^{BB,\rm PT} \approx 2.4 \times 10^{-7} \mu\text{K}^2 \,. \tag{A6}$$

With these numbers, we can now estimate the corresponding GW energy density $\Omega_{\rm GW}$ at this frequency. Before horizon re-entry, the GW energy density sourced by the inflationary signal is [90]

$$\Omega_{\rm GW}^{\rm inf} = \frac{\Omega_R}{24} \mathcal{P}_h^{\rm inf}(k) \,, \tag{A7}$$

where we have assumed radiation domination. Similarly, for phase transitions during radiation domination, we can combine Eqs. (31) and (39) to obtain

$$\Omega_{\rm GW}^{\rm PT} = \frac{\Omega_R}{3} \left(\frac{k}{a_* H_*} \right)^2 \mathcal{P}_h^{\rm PT}(k) \,, \tag{A8}$$

where $\Omega_R = \rho_R/\rho_{\rm tot}$ is the energy fraction of radiation. Thus, using $(a_* H_*)^{-1} = \tau_*$ and our model parameters to enforce $\mathcal{P}_h^{\rm inf} \approx \mathcal{P}_{\rm h}^{\rm PT}$ at k_{100}, the gravitational wave from phase transition has a smaller energy density receives an IR suppression $(k\tau_*)^2$ compared to the inflation signal

$$\Omega_{\rm GW}^{\rm PT} \sim (k_{100}\tau_*)^2 \Omega_{\rm GW}^{\rm inf} \,. \tag{A9}$$

For $T_* = 40$ keV the phase transition occurs at conformal time $\tau_* \approx 3 \times 10^{-3}$ Mpc, so at $f \approx 10^{-17}$ Hz, the ratio of signals from the two scenarios satisfies

$$\frac{\Omega_{\rm GW}^{\rm PT}}{\Omega_{\rm GW}^{\rm inf}} \sim (k_{100}\tau_*)^2 \sim 10^{-10} \,. \tag{A10}$$

This relative suppression is manifest as the difference between the GW spectra shown in Fig. 3 at this frequency. Importantly, Eq. (A9) also implies that the CMB B-mode constraints, when translated into the $\Omega_{\rm GW}$ parameter space, depend on the spectral shape of the source and must be recalculated using a dedicated analysis for each case; however, doing so for the phase transition signal is beyond the scope of this work.

Appendix B: Single and Double Bubble Spectra

Here we reproduce the explicit form for the function Δ from Eq. (30) derived originally in Ref. [55] working in the thin-wall and envelope approximations. As in this work, for simplicity we presume a luminal wall velocity $v_w = 1$, though the generalization to $v_w < 1$ is straightforward. We also set $\beta = 1$ for convenience and restore it later as needed using dimensional analysis. We parametrize this function according to $\Delta = \Delta^{(1)} + \Delta^{(2)}$, where the $\Delta^{(1),(2)}$ are the "single-bubble" and "double-bubble" contributions, respectively.

The "single-bubble" term arises when the bubble wall segments passing through two distinct points originate from the same nucleation event, where

$$\Delta^{(1)} = \frac{k^3}{12\pi} \int_0^\infty dy \int_y^\infty \frac{dr}{r^3} \frac{e^{-r/2}\cos(ky)}{\mathcal{I}(y,r)} \mathcal{G}(y,r,k), \tag{B1}$$

where the integrand depends on the functions

$$\mathcal{I}(y,r) = e^{y/r} + e^{-y/r} + \frac{y^2 - (r^2+4r)}{4r} e^{-r/2}, \tag{B2}$$

$$\mathcal{G}(y,r,k) = j_0(kr) F_0 + \frac{j_1(kr)}{kr} F_1 + \frac{j_2(kr)}{(kr)^2} F_2, \tag{B3}$$

and we have defined

$$F_0(y,r) = 2(r^2-y^2)^2(r^2+6r+12) \tag{B4}$$

$$F_1(y,r) = 2(r^2-y^2)[-r^2(r^3+4r^2+12r+24) + y^2(r^3+12r^2+60r+120)] \tag{B5}$$

$$F_2(y,r) = \frac{1}{2}\big[r^4(r^4+4r^3+20r^2+72r+144) - 2y^2r^2(r^4+12r^3+84r^2+360r+720) + y^4(r^4+20r^3+180r^2+840r+1680)\big]. \tag{B6}$$

The "double-bubble" contribution also arises from bubble wall segments passing through two spatial points, but in this case the two wall segments originate from distinct nucleation events and

$$\Delta^{(2)} = \frac{k^3}{96\pi} \int_0^\infty dy \int_y^\infty \frac{dr\cos(ky) j_2(kr) g(y,r) g(-y,r)}{r^4 \mathcal{I}(y,r)^2 (kr)^2}, \tag{B7}$$

where we have defined

$$g(y,r) = (r^2-y^2)[(r^3+2r^2)+y(r^2+6r+12)]e^{-r/2} \,. \tag{B8}$$

[1] D. Baumann, "Inflation," in *Theoretical Advanced Study Institute in Elementary Particle Physics: Physics of the Large and the Small*, pp. 523–686. 2011. arXiv:0907.5424 [hep-th].

[2] J. Ellis and D. Wands, "Inflation (2023)," arXiv:2312.13238 [astro-ph.CO].

[3] A. Kosowsky, "Cosmic microwave background polarization," *Annals Phys.* **246** (1996) 49–85, arXiv:astro-ph/9501045.

[4] M. Kamionkowski, A. Kosowsky, and A. Stebbins, "A Probe of primordial gravity waves and vorticity," *Phys. Rev. Lett.* **78** (1997) 2058–2061, arXiv:astro-ph/9609132.

[5] U. Seljak and M. Zaldarriaga, "Signature of gravity waves in polarization of the microwave background," *Phys. Rev. Lett.* **78** (1997) 2054–2057, arXiv:astro-ph/9609169.

[6] M. Kamionkowski, A. Kosowsky, and A. Stebbins, "Statistics of cosmic microwave background polarization," *Phys. Rev. D* **55** (1997) 7368–7388, arXiv:astro-ph/9611125.

[7] M. Zaldarriaga and U. Seljak, "An all sky analysis of polarization in the microwave background," *Phys. Rev. D* **55** (1997) 1830–1840, arXiv:astro-ph/9609170.

[8] U. Seljak, "Measuring polarization in cosmic microwave background," *Astrophys. J.* **482** (1997) 6, arXiv:astro-ph/9608131.

[9] W. Hu and M. J. White, "A CMB polarization primer," *New Astron.* **2** (1997) 323, arXiv:astro-ph/9706147.

[10] S. Dodelson, E. Rozo, and A. Stebbins, "Primordial gravity waves and weak lensing," *Phys. Rev. Lett.* **91** (2003) 021301, arXiv:astro-ph/0301177.

[11] T. L. Smith, M. Kamionkowski, and A. Cooray, "Direct detection of the inflationary gravitational wave background," *Phys. Rev. D* **73** (2006) 023504, arXiv:astro-ph/0506422.

[12] M. J. Mortonson, C. Dvorkin, H. V. Peiris, and W. Hu, "CMB polarization features from inflation versus reionization," *Phys. Rev. D* **79** (2009) 103519, arXiv:0903.4920 [astro-ph.CO].

[13] M. Kamionkowski and E. D. Kovetz, "The Quest for B Modes from Inflationary Gravitational Waves," *Ann. Rev. Astron. Astrophys.* **54** (2016) 227–269, arXiv:1510.06042 [astro-ph.CO].

[14] M. C. Guzzetti, N. Bartolo, M. Liguori, and S. Matarrese, "Gravitational waves from inflation," *Riv. Nuovo Cim.* **39** no. 9, (2016) 399–495, arXiv:1605.01615 [astro-ph.CO].

[15] S. Weinberg, "Damping of tensor modes in cosmology," *Phys. Rev. D* **69** (2004) 023503, arXiv:astro-ph/0306304.

[16] R. Flauger and S. Weinberg, "Tensor Microwave Background Fluctuations for Large Multipole Order," *Phys. Rev. D* **75** (2007) 123505, arXiv:astro-ph/0703179.

[17] D. Baumann, D. Green, and R. A. Porto, "B-modes and the Nature of Inflation," *JCAP* **01** (2015) 016, arXiv:1407.2621 [hep-th].

[18] **BICEP2** Collaboration, P. A. R. Ade *et al.*, "Detection of B-Mode Polarization at Degree Angular Scales by BICEP2," *Phys. Rev. Lett.* **112** no. 24, (2014) 241101, arXiv:1403.3985 [astro-ph.CO].

[19] M. Geller, S. Lu, and Y. Tsai, "B modes from postinflationary gravitational waves sourced by axionic instabilities at cosmic reionization," *Phys. Rev. D* **104** no. 8, (2021) 083517, arXiv:2104.08284 [hep-ph].

[20] A. Kosowsky, M. S. Turner, and R. Watkins, "Gravitational waves from first order cosmological phase transitions," *Phys. Rev. Lett.* **69** (1992) 2026–2029.

[21] M. Kamionkowski, A. Kosowsky, and M. S. Turner, "Gravitational radiation from first order phase transitions," *Phys. Rev. D* **49** (1994) 2837–2851, arXiv:astro-ph/9310044.

[22] A. Kosowsky, A. Mack, and T. Kahniashvili, "Gravitational radiation from cosmological turbulence," *Phys. Rev. D* **66** (2002) 024030, arXiv:astro-ph/0111483.

[23] R. Apreda, M. Maggiore, A. Nicolis, and A. Riotto, "Gravitational waves from electroweak phase transitions," *Nucl. Phys. B* **631** (2002) 342–368, arXiv:gr-qc/0107033.

[24] A. Nicolis, "Relic gravitational waves from colliding bubbles and cosmic turbulence," *Class. Quant. Grav.* **21** (2004) L27, arXiv:gr-qc/0303084.

[25] C. Grojean and G. Servant, "Gravitational Waves from Phase Transitions at the Electroweak Scale and Beyond," *Phys. Rev. D* **75** (2007) 043507, arXiv:hep-ph/0607107.

[26] S. J. Huber and T. Konstandin, "Gravitational Wave Production by Collisions: More Bubbles," *JCAP* **09** (2008) 022, arXiv:0806.1828 [hep-ph].

[27] T. Kahniashvili, A. Kosowsky, G. Gogoberidze, and Y. Maravin, "Detectability of Gravitational Waves from Phase Transitions," *Phys. Rev. D* **78** (2008) 043003, arXiv:0806.0293 [astro-ph].

[28] T. Kahniashvili, L. Kisslinger, and T. Stevens, "Gravitational Radiation Generated by Magnetic Fields in Cosmological Phase Transitions," *Phys. Rev. D* **81** (2010) 023004, arXiv:0905.0643 [astro-ph.CO].

[29] C. Caprini, R. Durrer, T. Konstandin, and G. Servant, "General Properties of the Gravitational Wave Spectrum from Phase Transitions," *Phys. Rev. D* **79** (2009) 083519, arXiv:0901.1661 [astro-ph.CO].

[30] J. R. Espinosa, T. Konstandin, J. M. No, and G. Servant, "Energy Budget of Cosmological First-order Phase Transitions," *JCAP* **06** (2010) 028, arXiv:1004.4187 [hep-ph].

[31] M. Hindmarsh, S. J. Huber, K. Rummukainen, and D. J. Weir, "Gravitational waves from the sound of a first order phase transition," *Phys. Rev. Lett.* **112** (2014) 041301, arXiv:1304.2433 [hep-ph].

[32] C. Caprini *et al.*, "Science with the space-based interferometer eLISA. II: Gravitational waves from cosmological phase transitions," *JCAP* **04** (2016) 001, arXiv:1512.06239 [astro-ph.CO].

[33] C. Caprini, "Stochastic background of gravitational waves from cosmological sources," *J. Phys. Conf. Ser.* **610** no. 1, (2015) 012004, arXiv:1501.01174 [gr-qc].

[34] L. Kisslinger and T. Kahniashvili, "Polarized Gravitational Waves from Cosmological Phase Transitions," *Phys. Rev. D* **92** no. 4, (2015) 043006, arXiv:1505.03680 [astro-ph.CO].

[35] M. Hindmarsh, S. J. Huber, K. Rummukainen, and D. J. Weir, "Numerical simulations of acoustically generated gravitational waves at a first order phase transition," *Phys. Rev. D* **92** no. 12, (2015) 123009, arXiv:1504.03291 [astro-ph.CO].

[36] P. Schwaller, "Gravitational Waves from a Dark Phase Transition," *Phys. Rev. Lett.* **115** no. 18, (2015) 181101, arXiv:1504.07263 [hep-ph].

[37] P. S. B. Dev and A. Mazumdar, "Probing the Scale of New Physics by Advanced LIGO/VIRGO," *Phys. Rev. D* **93** no. 10, (2016) 104001, arXiv:1602.04203 [hep-ph].

[38] R. Jinno and M. Takimoto, "Gravitational waves from bubble dynamics: Beyond the Envelope," *JCAP* **01** (2019) 060, arXiv:1707.03111 [hep-ph].

[39] M. Hindmarsh, S. J. Huber, K. Rummukainen, and D. J. Weir, "Shape of the acoustic gravitational wave power spectrum from a first order phase transition," *Phys. Rev. D* **96** no. 10, (2017) 103520, arXiv:1704.05871 [astro-ph.CO]. [Erratum: Phys.Rev.D 101, 089902 (2020)].

[40] D. J. Weir, "Gravitational waves from a first order electroweak phase transition: a brief review," *Phil. Trans. Roy. Soc. Lond. A* **376** no. 2114, (2018) 20170126, arXiv:1705.01783 [hep-ph]. [Erratum: Phil.Trans.Roy.Soc.Lond.A 381, 20230212 (2023)].

[41] V. Brdar, A. J. Helmboldt, and J. Kubo, "Gravitational Waves from First-Order Phase Transitions: LIGO as a Window to Unexplored Seesaw Scales," *JCAP* **02** (2019) 021, arXiv:1810.12306 [hep-ph].

[42] C. Caprini and D. G. Figueroa, "Cosmological Backgrounds of Gravitational Waves," *Class. Quant. Grav.* **35** no. 16, (2018) 163001, arXiv:1801.04268 [astro-ph.CO].

[43] A. Mazumdar and G. White, "Review of cosmic phase transitions: their significance and experimental signatures," *Rept. Prog. Phys.* **82** no. 7, (2019) 076901, arXiv:1811.01948 [hep-ph].

[44] D. Cutting, M. Hindmarsh, and D. J. Weir, "Gravitational waves from vacuum first-order phase transitions: from the envelope to the lattice," *Phys. Rev. D* **97** no. 12, (2018) 123513, arXiv:1802.05712 [astro-ph.CO].

[45] M. Geller, A. Hook, R. Sundrum, and Y. Tsai, "Primordial Anisotropies in the Gravitational Wave Background from Cosmological Phase Transitions," *Phys. Rev. Lett.* **121** no. 20, (2018) 201303, arXiv:1803.10780 [hep-ph].

[46] T. Alanne, T. Hugle, M. Platscher, and K. Schmitz, "A fresh look at the gravitational-wave signal from cosmological phase transitions," *JHEP* **03** (2020) 004, arXiv:1909.11356 [hep-ph].

[47] M. Hindmarsh and M. Hijazi, "Gravitational waves from first order cosmological phase transitions in the Sound Shell Model," *JCAP* **12** (2019) 062, arXiv:1909.10040 [astro-ph.CO].

[48] K. Schmitz, "New Sensitivity Curves for Gravitational-Wave Signals from Cosmological Phase Transitions," *JHEP* **01** (2021) 097, arXiv:2002.04615 [hep-ph].

[49] M. B. Hindmarsh, M. Lüben, J. Lumma, and M. Pauly, "Phase transitions in the early universe," *SciPost Phys. Lect. Notes* **24** (2021) 1, arXiv:2008.09136 [astro-ph.CO].

[50] J. Ellis, M. Lewicki, and J. M. No, "Gravitational waves from first-order cosmological phase transitions: lifetime of the sound wave source," *JCAP* **07** (2020) 050, arXiv:2003.07360 [hep-ph].

[51] D. Cutting, E. G. Escartin, M. Hindmarsh, and D. J. Weir, "Gravitational waves from vacuum first order phase transitions II: from thin to thick walls," *Phys. Rev. D* **103** no. 2, (2021) 023531, arXiv:2005.13537 [astro-ph.CO].

[52] P. Athron, C. Balázs, A. Fowlie, L. Morris, and L. Wu, "Cosmological phase transitions: From perturbative particle physics to gravitational waves," *Prog. Part. Nucl. Phys.* **135** (2024) 104094, arXiv:2305.02357 [hep-ph].

[53] C. Caprini, R. Jinno, T. Konstandin, A. Roper Pol, H. Rubira, and I. Stomberg, "Gravitational waves from decaying sources in strong phase transitions," arXiv:2409.03651 [gr-qc].

[54] C. Caprini, R. Durrer, and G. Servant, "Gravitational wave generation from bubble collisions in first-order phase transitions: An analytic approach," *Phys. Rev. D* **77** (2008) 124015, arXiv:0711.2593 [astro-ph].

[55] R. Jinno and M. Takimoto, "Gravitational waves from bubble collisions: An analytic derivation," *Phys. Rev. D* **95** no. 2, (2017) 024009, arXiv:1605.01403 [astro-ph.CO].

[56] C. Caprini and D. G. Figueroa, "Cosmological Backgrounds of Gravitational Waves," *Class. Quant. Grav.* **35** no. 16, (2018) 163001, arXiv:1801.04268 [astro-ph.CO].

[57] G. Elor, R. Jinno, S. Kumar, R. McGehee, and Y. Tsai, "Finite Bubble Statistics Constrain Late Cosmological Phase Transitions," arXiv:2311.16222 [hep-ph].

[58] J. Lesgourgues, "The Cosmic Linear Anisotropy Solving System (CLASS) I: Overview," arXiv:1104.2932 [astro-ph.IM].

[59] D. Blas, J. Lesgourgues, and T. Tram, "The Cosmic Linear Anisotropy Solving System (CLASS) II: Approximation schemes," *JCAP* **07** (2011) 034, arXiv:1104.2933 [astro-ph.CO].

[60] V. A. Rubakov and D. S. Gorbunov, *Introduction to the Theory of the Early Universe: Hot big bang theory*. World Scientific, Singapore, 2017.

[61] T. Kite, J. Chluba, A. Ravenni, and S. P. Patil, "Clarifying transfer function approximations for the large-scale gravitational wave background in ΛCDM," *Mon. Not. Roy. Astron. Soc.* **509** no. 1, (2021) 1366–1376, arXiv:2107.13351 [astro-ph.CO].

[62] S. W. Hawking, I. G. Moss, and J. M. Stewart, "Bubble Collisions in the Very Early Universe," *Phys. Rev. D* **26** (1982) 2681.

[63] A. Kosowsky and M. S. Turner, "Gravitational radiation from colliding vacuum bubbles: envelope approximation to many bubble collisions," *Phys. Rev. D* **47** (1993) 4372–4391, arXiv:astro-ph/9211004.

[64] M. Hindmarsh, "Sound shell model for acoustic gravitational wave production at a first-order phase transition in the early Universe," *Phys. Rev. Lett.* **120** no. 7, (2018) 071301, arXiv:1608.04735 [astro-ph.CO].

[65] A. Roper Pol, S. Procacci, and C. Caprini, "Characterization of the gravitational wave spectrum from sound waves within the sound shell model," *Phys. Rev. D* **109** no. 6, (2024) 063531, arXiv:2308.12943

[gr-qc].
[66] C. Caprini and R. Durrer, "Gravitational waves from stochastic relativistic sources: Primordial turbulence and magnetic fields," *Phys. Rev. D* **74** (2006) 063521, arXiv:astro-ph/0603476.
[67] T. Kahniashvili, L. Campanelli, G. Gogoberidze, Y. Maravin, and B. Ratra, "Gravitational Radiation from Primordial Helical Inverse Cascade MHD Turbulence," *Phys. Rev. D* **78** (2008) 123006, arXiv:0809.1899 [astro-ph]. [Erratum: Phys.Rev.D 79, 109901 (2009)].
[68] C. Caprini, R. Durrer, and G. Servant, "The stochastic gravitational wave background from turbulence and magnetic fields generated by a first-order phase transition," *JCAP* **12** (2009) 024, arXiv:0909.0622 [astro-ph.CO].
[69] P. Auclair, C. Caprini, D. Cutting, M. Hindmarsh, K. Rummukainen, D. A. Steer, and D. J. Weir, "Generation of gravitational waves from freely decaying turbulence," *JCAP* **09** (2022) 029, arXiv:2205.02588 [astro-ph.CO].
[70] A. Hook, G. Marques-Tavares, and D. Racco, "Causal gravitational waves as a probe of free streaming particles and the expansion of the Universe," *JHEP* **02** (2021) 117, arXiv:2010.03568 [hep-ph].
[71] **Planck** Collaboration, N. Aghanim *et al.*, "Planck 2018 results. VI. Cosmological parameters," *Astron. Astrophys.* **641** (2020) A6, arXiv:1807.06209 [astro-ph.CO]. [Erratum: Astron.Astrophys. 652, C4 (2021)].
[72] U. Seljak, "Gravitational lensing effect on cosmic microwave background anisotropies: A Power spectrum approach," *Astrophys. J.* **463** (1996) 1, arXiv:astro-ph/9505109.
[73] F. Bernardeau, "Weak lensing detection in CMB maps," *Astron. Astrophys.* **324** (1997) 15–26, arXiv:astro-ph/9611012.
[74] M. Zaldarriaga and U. Seljak, "Gravitational lensing effect on cosmic microwave background polarization," *Phys. Rev. D* **58** (1998) 023003, arXiv:astro-ph/9803150.
[75] W. Hu and T. Okamoto, "Mass reconstruction with cmb polarization," *Astrophys. J.* **574** (2002) 566–574, arXiv:astro-ph/0111606.
[76] W. Hu, "Dark synergy: Gravitational lensing and the CMB," *Phys. Rev. D* **65** (2002) 023003, arXiv:astro-ph/0108090.
[77] W. Hu, M. M. Hedman, and M. Zaldarriaga, "Benchmark parameters for CMB polarization experiments," *Phys. Rev. D* **67** (2003) 043004, arXiv:astro-ph/0210096.
[78] U. Seljak and C. M. Hirata, "Gravitational lensing as a contaminant of the gravity wave signal in CMB," *Phys. Rev. D* **69** (2004) 043005, arXiv:astro-ph/0310163.
[79] A. Lewis and A. Challinor, "Weak gravitational lensing of the CMB," *Phys. Rept.* **429** (2006) 1–65, arXiv:astro-ph/0601594.
[80] D. Hanson, A. Challinor, and A. Lewis, "Weak lensing of the CMB," *Gen. Rel. Grav.* **42** (2010) 2197–2218, arXiv:0911.0612 [astro-ph.CO].
[81] S. Dodelson, "Cross-Correlating Probes of Primordial Gravitational Waves," *Phys. Rev. D* **82** (2010) 023522, arXiv:1001.5012 [astro-ph.CO].
[82] S. C. Hotinli, J. Meyers, C. Trendafilova, D. Green, and A. van Engelen, "The benefits of CMB delensing," *JCAP* **04** no. 04, (2022) 020, arXiv:2111.15036 [astro-ph.CO].
[83] C. Trendafilova, S. C. Hotinli, and J. Meyers, "Improving constraints on inflation with CMB delensing," *JCAP* **06** (2024) 017, arXiv:2312.02954 [astro-ph.CO].
[84] S. Bird, H. V. Peiris, M. Viel, and L. Verde, "Minimally parametric power spectrum reconstruction from the Lyman α forest," *MNRAS* **413** no. 3, (May, 2011) 1717–1728, arXiv:1010.1519 [astro-ph.CO].
[85] **Planck** Collaboration, Y. Akrami *et al.*, "Planck 2018 results. X. Constraints on inflation," *Astron. Astrophys.* **641** (2020) A10, arXiv:1807.06211 [astro-ph.CO].
[86] D. J. Fixsen and J. C. Mather, "The spectral results of the far-infrared absolute spectrophotometer instrument on cobe," *The Astrophysical Journal* **581** no. 2, (Dec, 2002) 817. https://dx.doi.org/10.1086/344402.
[87] J. Chluba, R. Khatri, and R. A. Sunyaev, "CMB at 2x2 order: The dissipation of primordial acoustic waves and the observable part of the associated energy release," *Mon. Not. Roy. Astron. Soc.* **425** (2012) 1129–1169, arXiv:1202.0057 [astro-ph.CO].
[88] **LiteBIRD** Collaboration, E. Allys *et al.*, "Probing Cosmic Inflation with the LiteBIRD Cosmic Microwave Background Polarization Survey," *PTEP* **2023** no. 4, (2023) 042F01, arXiv:2202.02773 [astro-ph.IM].
[89] **CMB-S4** Collaboration, K. N. Abazajian *et al.*, "CMB-S4 Science Book, First Edition," arXiv:1610.02743 [astro-ph.CO].
[90] P. D. Lasky *et al.*, "Gravitational-wave cosmology across 29 decades in frequency," *Phys. Rev. X* **6** no. 1, (2016) 011035, arXiv:1511.05994 [astro-ph.CO].
[91] **BICEP, Keck** Collaboration, P. A. R. Ade *et al.*, "Improved Constraints on Primordial Gravitational Waves using Planck, WMAP, and BICEP/Keck Observations through the 2018 Observing Season," *Phys. Rev. Lett.* **127** no. 15, (2021) 151301, arXiv:2110.00483 [astro-ph.CO].
[92] **LISA** Collaboration, P. Amaro-Seoane *et al.*, "Laser Interferometer Space Antenna," arXiv:1702.00786 [astro-ph.IM].
[93] G. Janssen *et al.*, "Gravitational wave astronomy with the SKA," *PoS* **AASKA14** (2015) 037, arXiv:1501.00127 [astro-ph.IM].
[94] A. Kogut *et al.*, "The Primordial Inflation Explorer (PIXIE): Mission Design and Science Goals," arXiv:2405.20403 [astro-ph.CO].
[95] A. Sabyr, C. Sierra, J. C. Hill, and J. J. McMahon, "SPECTER: An Instrument Concept for CMB Spectral Distortion Measurements with Enhanced Sensitivity," arXiv:2409.12188 [astro-ph.CO].